Synthesis of Rhodium, Iridium, and Palladium Tetranuclear Complexes Directed by 2,6-Dimercaptopyridine. X-ray Crystal Structure of $[Rh_4(\mu\text{-}PyS_2)_2(cod)_4]$ (cod = 1,5-Cyclooctadiene)

Jesús J. Pérez-Torrente, Miguel A. Casado, Miguel A. Ciriano,* Fernando J. Lahoz, and Luis A. Oro*

Departamento de Química Inorgánica, Instituto de Ciencia de Materiales de Aragón, Universidad de Zaragoza-CSIC, 50009 Zaragoza, Spain

Received July 7, 1995[⊗]

Tetranuclear diolefin complexes of the general formula $[M_4(\mu_4\text{-}PyS_2)_2(diolefin)_4]$ [M = Rh, diolefin = 1,5-cyclooctadiene (cod) (**1**), 2,5-norbornadiene (nbd) (**2**), tetrafluorobenzobarrelene (tfbb) (**3**); M = Ir, diolefin = cod (**4**), PyS_2 = 2,6-pyridinedithiolate) are prepared in high yield by reaction of the appropriate complex $[\{M(\mu\text{-}Cl)(diolefin)\}_2]$ with the salt Li_2PyS_2 generated "in situ". This method is also used to prepare $[Pd_4(\mu\text{-}PyS_2)_2(allyl)_4]$ (**5**). Alternative syntheses for these complexes are also described. The structure of **1** was conclusively determined by a single-crystal X-ray analysis. Complex **1** crystallizes in the monoclinic system, space group *C2/c*, with $a = 10.252(1)$ Å, $b = 17.023(2)$ Å, $c = 23.114(3)$ Å, $\beta = 99.50(1)°$, and $Z = 4$. Refinement by full matrix least-squares gave final $R = 0.028$ and $R_w = 0.024$. Complex **1** is tetranuclear with two S,N,S-tridentate 2,6-dimercaptopyridine ligands bridging all of the four metallic centers and presents a crystallographically imposed C_2 symmetry relating two "$Rh_2(\mu_4\text{-}PyS_2)(cod)_2$" moieties. The two S atoms of each bridging ligand exhibit different coordination modes; while one is bonded to one metal, the second one is coordinated to two different rhodium centers. The shortest Rh···Rh separation is 3.1435(5) Å. Carbonylation of the rhodium diolefin complexes under atmospheric pressure gives $[Rh_4(\mu_4\text{-}PyS_2)_2(CO)_8]$ (**6**) which maintains the molecular framework of **1**. Further reaction of the carbonyl complex with PPh_3 gives $[Rh_4(\mu\text{-}PyS_2)_2(CO)_4(PPh_3)_4]$ (**7**), but this complex is prepared more conveniently by reaction of Li_2PyS_2 with $[\{Rh(\mu\text{-}Cl)(CO)(PPh_3)\}_2]$. The replacement of CO by PPh_3 is not selective, and this complex exists in solution as a mixture of three isomers due to the relative position of the PPh_3 groups. The diolefinic and carbonyl complexes are fluxional. Variable temperature ^1H and $^{13}C\{^1H\}$ spectra associated with H,H-COSY experiments led to the assignment of the olefinic resonances and the conclusion that the two diolefins at the inner part of the complexes are rigid, while the two external ones undergo the fluxional behavior due to an inversion at the terminal sulfur donor atoms. This is also the origin of the fluxionality of the carbonyl complex. Deprotonation of $Py(SH)_2$ with [Rh(acac)(cod)] (acac = acetylacetonate) can be carried out stepwise, giving the dinuclear complex $[Rh_2(\mu\text{-}PyS_2H)_2(cod)_2]$ (**8**), and later the tetranuclear complex **1**. This method to synthesize heterotetranuclear complexes by the addition of either [Ir(acac)(cod)] or $[\{Ir(\mu\text{-}OMe)(cod)\}_2]$ to the isolated dinuclear rhodium complex (**8**) has been shown to be nonselective, giving a mixture of tetranuclear complexes with the $[Rh_3Ir]^{4+}$, $[Rh_2Ir_2]^{4+}$, and $[RhIr_3]^{4+}$ cores. The rhodium complexes undergo two reversible one-electron oxidations at a platinum bead electrode in dichloromethane separated by approximately 0.4 V at potentials $E°$ in the ranges 0.0−0.4 and 0.4−0.8 V. The electrochemical behavior of the iridium complex is more complicated, undergoing two similar one-electron oxidations followed by a chemical reaction.

Introduction

The synthesis, reactivity, and structural characterization of di- and polynuclear complexes has received considerable attention due to their potential for novel stoichiometric and catalytic reactions.[1] Bidentate bridging ligands such as bis(diphenylphosphino)methane (dppm) and 2-(diphenylphosphino)pyridine (**A**) (Chart 1) that contain a single bridgehead atom, have proven to be very effective in stabilizing molecules containing single or even multiple metal−metal bonds[2] due to the flexibility to adapt both to variations of metal−metal separation and to the coordination geometries about the two metal atoms.[3,4]

Chart 1

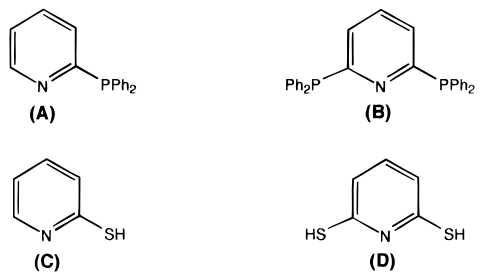

Going from dinuclear to polynuclear complexes generally requires the development of new synthetic strategies in which

⊗ Abstract published in *Advance ACS Abstracts,* February 15, 1996.

(1) (a) *The Chemistry of Metal Cluster Complexes*; Shriver, D. F., Kaesz, H. D., Adams, R. D., Eds.; VCH: New York, 1990. (b) *Comprehensive Organometallic Chemistry*; Abel, E. W., Stone, F. G. A., Wilkinson, G., Eds.; Pergamon: Oxford, England, 1982. (c) *Homogeneous Catalysis with Metal Phosphine Complexes*; Pignolet, L. H., Ed.; Plenum Press: New York, 1983. (d) Challoner, P. A.; Esteruelas, M. A.; Joó, F.; Oro, L. A. *Homogeneous Hydrogenation*; Kluwer: Dordretcht, The Netherlands, 1994.

(2) Cotton, F. A.; Walton, R. A. *Multiple Bonds between Metal Atoms*; Wiley: New York, 1993.

(3) (a) Puddephatt, R. J. *J. Chem. Soc. Rev.* **1983**, 99. (b) Chaudret, B.; Delavaux, B.; Poilblanc, R. *Coord. Chem. Rev.* **1988**, *86*, 191.

(4) Newkome, G. R. *Chem. Rev.* **1993**, *93*, 2067. Arena, C. G.; Ciani, G.; Drommi, D.; Faraone, F.; Proserpio, D. M.; Rotondo, E. *J. Organomet. Chem.* **1994**, *484*, 71, and references cited therein.

0020-1669/96/1335-1782$12.00/0

the design of the bridging ligands plays an important role: an increase of the number of donor atoms in the bridging ligands and the presence of several lone electron pairs (O or S for example) are useful alternatives.[5] In addition, the framework in which the donor atoms are placed should be carefully chosen to produce small "bites" and to avoid undesired coordination modes. Ligands of these characteristics are, for example, bis(diphenylphosphinomethyl)phenylphosphine (dpmp),[6] bis(diphenylphosphinomethyl)phenylarsine (dpam),[7] and 2,6-bis(diphenylphosphino)pyridine[4a,8] (**B**), which give rise to controlled synthesis of homo- and heterotrinuclear and tetranuclear complexes.[8] Other attempts to obtain complexes of high nuclearity by using polydentate ligands such as 7-diphenylphosphino-2,4-dimethyl-1,8-naphthyridine[9] and 2-mercapto-7-methyl-1,8-naphthyridine[10] have met little success so far, since only dinuclear complexes have been isolated. For synthetical purposes the bridging ligands should expand several metal atoms, as found in tetranuclear Mo−Pd complexes of 6-(diphenylphosphino)-2-pyridonate.[11]

We have shown that anionic bidentate ligands having a small bite and a structural donor unit N−C−S, like pyridine-2-thiolate (**C**) or benzothiazole-2-thiolate, are useful in building homo- and hetero-dinuclear complexes.[5e,12] Some of them behave as eight-membered metallomacrocycles, where a third metallic fragment can be trapped giving rise to homo- and heterotrinuclear aggregates having the framework $[M_3(\mu\text{-NCS})_2]$ of predetermined structure in a controlled way.[13] In this context, 2,6-dimercaptopyridine (**D**) is a new system which has not been investigated previously. The doubly thiolate functionalized pyridine ligand should combine the features shown by other 2,6-difunctionalized pyridine derivatives and those of the thione or thiolate ligands. Therefore, it may interact with transition metals in a particularly, attractive manner, with regard to the ability to build polynuclear aggregates. We report here the synthesis and structure of new tetranuclear complexes of rhodium(I), iridium(I), and palladium(II) supported by 2,6-dimercaptopyridine (**D**) and their electrochemical properties.

Experimental Section

General. All manipulations were performed under a dry nitrogen atmosphere using Schlenk-tube techniques. Solvents were dried by standard methods and distilled under nitrogen immediately prior to use. Standard literature procedures were used to prepare the starting materials $[\{Rh(\mu\text{-Cl})(\text{diolefin})\}_2]$ (diolefin = cod,[14] nbd[15]), $[\{Rh(\mu\text{-Cl})(CO)(PPh_3)\}_2]$,[16] and $[\{Pd(\mu\text{-Cl})(\text{allyl})\}_2]$.[17] The acetylacetonate complexes [Ir(acac)(cod)] and $[Rh(acac)(CO)(PPh_3)]$ were prepared following the procedure described for [Rh(acac)(cod)],[18] and the complexes $[\{Rh(\mu\text{-OMe})(\text{cod})\}_2]$ and $[\{Ir(\mu\text{-OMe})(\text{cod})\}_2]$ were prepared according to the method reported for $[\{Rh(\mu\text{-OMe})(\text{tfbb})\}_2]$.[19] $AgBF_4$ was purchased from Fluka Chemicals and used as received. 2,6-Dimercaptopyridine $[Py(SH)_2]$ was synthesized as described by Pappalardo et al.[20] using the modified method of Vögtle and Effler.[21] The NMR spectra of 2,6-dimercaptopyridine are as follows. ^{1}H NMR (toluene-d_8, 215 K): δ 15.61 (s, 1H, SH), 9.43 (s, 1H, NH), 6.75 (d, 1H, 8.2 Hz), 6.02 (dd, 1H, 8.2 and 7.2 Hz), 5.89 (d, 1H, 7.2 Hz). ^{1}H NMR spectrum ($CDCl_3$, 293 K): δ 9.56 (br, 2H, SH), 7.25 (t, 8.0 Hz, 1H), 6.95 (d, 2H, 8.0 Hz). $^{13}C\{^1H\}$ NMR spectrum ($CDCl_3$, 328 K): δ 160.8 (CS), 137.8, 121.8 (2C).

Physical Measurements. ^{1}H, $^{13}C\{^1H\}$, and $^{31}P\{^1H\}$ NMR spectra were recorded on Varian UNITY 300 and Bruker ARX 300 spectrometers operating at 299.95 and 300.13; 75.42 and 75.47; 121.42 and 121.49 MHz, respectively. Chemical shifts are reported in parts per million and referenced to Me_4Si using the signal of the deuterated solvent (^{1}H and ^{13}C) and 85% H_3PO_4 (^{31}P) as external reference, respectively. IR spectra were recorded on a Perkin-Elmer 783 spectrometer using Nujol mulls between polyethylene sheets or in solution in a cell with NaCl windows. Elemental analyses were performed with a Perkin-Elmer 240-C microanalyzer. Conductivities were measured in *ca*. 5×10^{-4} M dichloromethane solutions using a Philips PW 9501/01 conductimeter. Molecular weights were determined with a Knauer osmometer using chloroform solutions of the complexes. Mass spectra were recorded in a VG Autospec double-focusing mass spectrometer operating in the FAB^+ mode. Ions were produced with the standard Cs^+ gun at *ca*. 30 kV; 3-nitrobenzyl alcohol (NBA) was used as matrix.

Cyclic voltammetric experiments were performed with a EG&G PARC Model 273 potentiostat/galvanostat. A three-electrode glass cell consisting of a platinum-disk working electrode, a platinum-wire auxiliary electrode, and a standard calomel reference electrode (SCE) was used. Linear voltamperometry was performed by using a rotating platinum electrode (RDE) as the working electrode. Tetra-*n*-butylammonium hexafluorophosphate (TBAH) was employed as supporting electrolyte. Electrochemical experiments were carried out under nitrogen in *ca*. 5×10^{-4} M dichloromethane solutions of the complexes and 0.1 M in TBAH. The $[Fe(\eta\text{-}C_5H_5)_2]^+/[Fe(\eta\text{-}C_5H_5)_2]$ couple is observed at +0.47 V under these experimental conditions.

Preparation of the Complexes. $[Rh_4(\mu\text{-}PyS_2)_2(cod)_4]$ (1). Method A. To a solution of $[\{Rh(\mu\text{-OMe})(\text{cod})\}_2]$ (0.100 g, 0.206 mmol) in dichloromethane (15 mL), solid 2,6-dimercaptopyridine (0.029 g, 0.206 mmol) was added. The mixture was stirred for 30 min to give a deep red solution. Concentration of the solution under vacuum to 1 mL and addition of diethyl ether (5 mL) gave an orange microcrystalline

(5) (a) Dunbar, K. R.; Matonic, J. H.; Saharan, V. P. *Inorg. Chem.* **1994**, *33*, 25. (b) Cayton, R. H.; Chisholm, M. H.; Huffman, J. C.; Lobkovsky, E. B.; *Angew. Chem., Int. Ed. Engl.* **1991**, *30*, 862. (c) Cayton, R. H.; Chisholm, M. H.; Huffman, J. C.; Lobkovsky, E. B. *J. Am. Chem. Soc.* **1991**, *103*, 8709. (d) Ciriano, M. A.; Villarroya, B. E.; Oro, L. A. *Inorg. Chim. Acta* **1986**, *120*, 43. (e) Oro, L. A.; Ciriano, M. A.; Viguri, F.; Tiripicchio, A.; Tiripicchio-Camellini, M. *New J. Chem.* **1986**, *10*, 75.

(6) (a) Balch, A. L.; Linehan, J. C.; Olmstead, M. M. *Inorg. Chem.* **1986**, *25*, 3937. (b) Balch, A. L.; Fosset, L. A.; Guimerans, R. R.; Olmstead, M. M. *Organometallics* **1985**, *4*, 781. (c) Balch, A. L.; Guimerans, R. R.; Olmstead, M. M. *J. Organomet. Chem.* **1984**, *268*, C38. (d) Olmstead, M. M.; Guimerans, R. R.; Balch, A. L. *Inorg. Chem.* **1983**, *22*, 2473.

(7) (a) Balch, A. L.; Nagle, J. K.; Oram, D. E.; Reedy, P. E., Jr. *J. Am. Chem. Soc.* **1988**, *110*, 454. (b) Bailey, D. A.; Balch, A. L.; Fosset, L. A.; Olmstead, M. M.; Reedy, P. E., Jr. *Inorg. Chem.* **1987**, *26*, 2413. (c) Balch, A. L.; Oram, D. E.; Reedy, P. E., Jr. *Inorg. Chem.* **1987**, *26*, 1836. (d) Balch, A. L.; Nagle, J. K.; Olmstead, M. M.; Reedy, P. E., Jr. *J. Am. Chem. Soc.* **1987**, *109*, 4123. (e) Balch, A. L.; Fosset, L. A.; Olmstead, M. M.; Oram, D. E.; Reedy, P. E., Jr. *J. Am. Chem. Soc.* **1985**, *107*, 5272.

(8) Balch, A. L. *Prog. Inorg. Chem.* **1994**, *41*, 239.

(9) Lo Schiavo, S.; Grassi, M.; De Munno, G.; Nicolo, F.; Tresoldi, G. *Inorg. Chim. Acta* **1994**, *216*, 209.

(10) Sheldrick, W. S.; Mintert, M. *Inorg. Chim. Acta* **1994**, *219*, 23.

(11) Mashima, K.; Nakano, H.; Nakamura, A. *J. Am. Chem. Soc.* **1993**, *115*, 11632.

(12) (a) Ciriano, M. A.; Pérez-Torrente, J. J.; Lahoz, F. J.; Oro, L. A. *Inorg. Chem.* **1992**, *31*, 969. (b) Yap, G. P. A.; Jensen, C. M. *Inorg. Chem.* **1992**, *31*, 4823. (c) Reynolds, J. G.; Sendlinger, S. C.; Murray, A. M.; Huffman, J. C.; Christou, G. *Angew. Chem., Int. Ed. Engl.* **1992**, *31*, 1253. (d) Yamamoto, J. H.; Yoshida, W.; Jensen, C. M. *Inorg. Chem.* **1991**, *30*, 1353. (e) Ciriano, M. A.; Viguri, F.; Pérez-Torrente, J. J.; Lahoz, F. J.; Oro, L. A.; Tiripicchio, A.; Tiripicchio-Camellini, M. *J. Chem. Soc., Dalton Trans.* **1989**, 25.

(13) (a) Ciriano, M. A.; Pérez-Torrente, J. J.; Oro, L. A.; Tiripicchio, A.; Tiripicchio-Camellini, M. *J. Chem. Soc., Dalton Trans.* **1991**, 225. (b) Ciriano, M. A.; Pérez-Torrente, J. J.; Viguri, F.; Lahoz, F. J.; Oro, L. A.; Tiripicchio, A.; Tiripicchio-Camellini, M. *J. Chem. Soc., Dalton Trans.* **1990**, 1493. (c) Deeming, A. J.; Meah, M. N.; Bates, P. A.; Hursthouse, M. B. *J. Chem. Soc., Dalton Trans.* **1988**, 235. (d) Deeming, A. J.; Meah, M. N.; Bates, P. A.; Hursthouse, M. B. *J. Chem. Soc., Dalton Trans.* **1988**, 2139.

(14) Giordano, G.; Crabtree, R. H. *Inorg. Synth.* **1979**, *19*, 218.

(15) Abel, E. W., Bennett, M. A.; Wilkinson, G. *J. Chem. Soc.* **1959**, 3178.

(16) Steele, D. F.; Stephenson, T. A. *J. Chem. Soc., Dalton Trans.* **1972**, 2161.

(17) Tatsuno, Y.; Yoshida, T.; Otsuka, S. *Inorg. Synth.* **1979**, *19*, 220.

(18) Bonati, F.; Wilkinson, G. *J. Chem. Soc.* **1964**, 3156.

(19) Usón, R.; Oro, L. A.; Cabeza, J. A. *Inorg. Synth.* **1985**, *23*, 126.

(20) Bottino, F.; Casentino, S.; Cunsolo, S.; Pappalardo, S. *J. Heterocycl. Chem.* **1981**, *18*, 199.

(21) Vögtle, F.; Effler, A. H. *Chem. Ber.* **1969**, *102*, 3071.

solid. The resulting suspension was concentrated, and methanol (10 mL) was added in order to complete the precipitation. The solid was filtered off, washed with methanol, and vacuum dried. Yield: 0.112 g (96%). Anal. Calcd for $C_{42}H_{54}N_2Rh_4S_4$: C, 44.78; H, 4.83; N, 2.49. Found: C, 44.12; H, 4.79; N, 2.28. ^{1}H NMR (toluene-d_8, 293 K): δ 8.23 (dd, 2H, J_{HH} = 7.6 and 1.0 Hz), 6.73 (dd, 2H, J_{HH} = 8.0 and 1.0 Hz), 6.29 (t, 2H, J_{HH} = 7.8 Hz, PyS_2 ligands), 5.06 (m, 2H, =CH), 4.72 (m, 10H, =CH), 4.54 (m, 2H, =CH), 3.65 (m, 2H, =CH), 2.6−2.85 (m, 12H, CH_2), 2.0−2.2 (m, 8H, CH_2), 1.85−2.0 (m, 8H, CH_2), 1.5−1.7 (m, 4H, CH_2) (cod ligands). ^{13}C NMR ($CDCl_3$, 293 K): δ 169.3 (CS), 166.8 (CS), 134.5, 125.3, 124.3 (CH, Py), 87.5 (d, J_{RhC} = 11 Hz, =CH), 85.6 (d, J_{RhC} = 11 Hz, =CH), 78.9 (d, J_{RhC} = 12 Hz, 2C, =CH), 78.15 (d, J_{RhC} = 12 Hz, 3C, =CH), 75.9 (d, J_{RhC} = 12 Hz, =CH), 35.3, 33.0, 31.3 (2C), 30.4 (2C), 29.1, 28.2 (CH_2 cod). MS (FAB^+, CH_2Cl_2, *m*/*z*): 1126 (M^+, 100%), 1018 (M^+ − cod, 16%), 906 (M^+ − 2cod − 4H, 20%), 800 (M^+ − 3cod − 2H, 23%), 694 (M^+ − 4cod, 30%). MW ($CHCl_3$): calcd, 1126; found, 1125.

Method B. [{Rh(μ-Cl)(cod)}$_2$] (0.100 g, 0.203 mmol) was added to a yellow solution of Li_2PyS_2 (0.203 mmol), prepared by addition of *n*-butyllithium (0.25 mL, 1.61 M in hexane, 0.40 mmol) to a solution of 2,6-dimercaptopyridine (0.029 g, 0.203 mmol) in tetrahydrofuran (15 mL). An orange solution was immediately formed and stirred for 30 min. The solvent was removed under vacuum, and the residue was washed with methanol (3 × 10 mL) and then recrystallized from dichloromethane (1 mL) and methanol (10 mL) to give 0.108 g of **1** (yield: 95%).

Method C. [Rh(acac)(cod)] (0.100 g, 0.322 mmol) and 2,6-dimercaptopyridine (0.023 g, 0.161 mmol) were stirred in dichloromethane (15 mL) for 30 min to give an orange solution. Concentration of the solution and work-up as in method B gave 0.087 g of **1** (yield: 97%).

Method D. Solid 2,6-dimercaptopyridine (0.046 g, 0.322 mmol) was added to a solution of [Rh(acac)(cod)] (0.100 g, 0.322 mmol) in dichloromethane (15 mL) to give an orange solution. This was stirred for 30 min, and then NEt_3 (97 μL, 0.70 mmol, 0.73 g mL^{-1}) was added. The mixture was stirred for a further 1 h and then concentrated under vacuum to ca. 1 mL. Work-up as described in method B 0.086 g of **1** (yield: 95%).

Method E. [Rh(acac)(cod)] (0.100 g, 0.322 mmol) and 2,6-dimercaptopyridine (0.046 g, 0.322 mmol) were reacted in dichloromethane (15 mL) for 30 min. Solid [{Rh(μ-OMe)(cod)}$_2$] (0.078 g, 0.161 mmol) was added and the mixture stirred for 1 h. Concentration of the solution under vacuum and work-up as described in method B gave 0.085 g of **1** (yield: 94%).

[Rh$_4$(μ-PyS$_2$)$_2$(nbd)$_4$] (2) was prepared from [{Rh(μ-Cl)(nbd)}$_2$] (0.100 g, 0.217 mmol) and Li_2PyS_2 (0.217 mmol) in tetrahydrofuran (10 mL) by method B described above for **1**. The compound crystallized out in tetrahydrofuran and was isolated, after addition of methanol (10 mL), as a red purple solid, which was filtered, washed with methanol, and vacuum dried. Yield: 0.101 g (88%). Anal. Calcd for $C_{38}H_{38}N_2Rh_4S_4$: C, 42.95; H, 3.60; N, 2.64. Found: C, 42.45; H, 3.34; N, 2.59.

[Rh$_4$(μ-PyS$_2$)$_2$(tfbb)$_4$] (3) was prepared from [{Rh(μ-OMe)(tfbb}$_2$] (0.100 g, 0.138 mmol) and 2,6-dimercaptopyridine (0.020 g, 0.138 mmol) in dichloromethane (15 mL) following the method A described above for **1**. Dark red microcrystals were obtained by concentration of the solution and slow addition of methanol (10 mL). The crystals were isolated by filtration, washed with methanol, and vacuum dried. Yield: 0.092 g (83%). Anal. Calcd for $C_{58}H_{30}F_{16}N_2Rh_4S_4$: C, 43.57; H, 1.89; N, 1.75. Found: C, 43.14; H, 2.16; N, 1.86. ^{1}H NMR ($CDCl_3$, 293 K): 7.68 (d, 2H, J_{HH} = 9 Hz), 6.75 (t, 2H, J_{HH} = 9.2 Hz), 6.65 (d, 2H, J_{HH} = 9.2 Hz) (PyS_2 ligands), 5.75 (s, 6H, CH), 5.63 (m, 2H, CH), 4.41 (m, 2H, =CH), 4.34 (m, 2H, =CH), 4.27 (m, 8H, =CH), 4.10 (m, 2H, =CH), 3.32 (m, 2H, =CH) (tfbb ligands). MS (FAB^+, CH_2Cl_2, *m*/*z*): 1599 (M^+ + 1H, 100%), 1372 (M^+ − tfbb, 8%), 1146 (M^+ − 2tfbb, 5%), 1043 (M^+ − 2tfbb-Rh, 6%), 920 (M^+ − 3tfbb, 11%), 800 (M^+ − 2tfbb, − 2Rh − PyS_2 + 1H, 14%), 694 (M^+ − 4tfbb, 22%).

[Ir$_4$(μ-PyS$_2$)$_2$(cod)$_4$] (4) was prepared from [{Ir(μ-OMe)(cod)}$_2$] (0.100 g, 0.151 mmol) and 2,6-dimercaptopyridine (0.021 g, 0.151 mmol) in dichloromethane (10 mL). The method A described above for **1** was followed, but exclusively *n*-hexane was added at precipitating and washing agent. The compound was isolated by filtration as a dark red microcrystalline solid. Yield: 0.092 g (82%). Anal. Calcd for $C_{42}H_{54}Ir_4N_2S_4$: C, 33.99; H, 3.66; N, 1.88. Found: C, 34.17; H, 3.72; N, 1.89. ^{1}H NMR ($CDCl_3$, 223 K): δ 7.91 (d, 2H, J_{HH} = 7.4 Hz), 6.73 (t, 2H, J_{HH} = 7.6 Hz), 6.64 (d, 2H, J_{HH} = 7.8 Hz, PyS_2 ligands), 4.91 (m, 2H, =CH), 4.69 (m, 2H, =CH), 4.58 (m, 2H, =CH), 4.29 (m, 2H, =CH), 3.70 (m, 2H, =CH), 3.54 (m, 2H, =CH), 2.95 (m, 2H, =CH), 2.85 (m, 2H, =CH), 2.75 (m, 2H, CH_2), 2.53 (m, 2H, CH_2); 2.0−2.4 (set of m, 16H, CH_2), 1.95 (m, 2H, CH_2), 1.75 (m, 2H, CH_2), 1.35 (m, 8H, CH_2) (cod ligands). ^{13}C NMR ($CDCl_3$, 293 K): δ 169.0 (CS), 166.1 (CS), 135.5, 127.8, 125.9 (CH, py), 70.8, 69.5, 64.4 (br, 4C), 64.0, 60.5 (=CH cod), 36.9, 34.2, 33.7 (2C), 29.3 (2C), 28.8, 28.6 (CH_2 cod). MS (FAB^+, CH_2Cl_2, *m*/*z*): 1485 (M^+ + 1H, 53%), 1183 (M^+ − Ir − cod, 100%), 1073 (M^+ − Ir − 2cod − 2H, 27%), 964 (M^+ − Ir − 3cod − 3H, 36%), 885 (M^+ − 2Ir − 2cod + 1H, 25%), 743 (M^+ − 2Ir − 2cod − PyS_2 + 2H, 28%).

[Pd$_4$(μ-PyS$_2$)$_2$(allyl)$_4$] (5) was prepared by reaction of [{Pd(μ-Cl)(allyl)}$_2$] (0.100 g, 0.273 mmol) with Li_2PyS_2 (0.273 mmol) in tetrahydrofuran (10 mL) according to the method B described above for complex **1**. The resulting orange solution was stirred for 1 h and then concentrated under vacuum to *ca*. 1 mL. Slow addition of methanol (5 mL) and cooling to −15 °C gave the complex as an orange microcrystalline solid which was filtered, washed with cold methanol, and vacuum dried. Yield: 0.090 g (76%). Anal. Calcd for $C_{22}H_{26}N_2Pd_4S_4$: C, 30.29; H, 3.00; N, 3.21. Found: C, 30.41; H, 3.07; N, 3.48. ^{1}H NMR ($CDCl_3$, 293 K): δ 7.38 (m, 1H), 7.12 (m, 1H), 6.94 (m, 2H), 6.69 (m, 1H), 6.62 (m, 1H, PyS_2 ligands), 5.1−5.7 (4H), 3.5−4.3 (set of m, 8H, syn-H), 2.3−3.5 (set of m, 8H, anti-H, allyl ligands). MS (FAB^+, THF, *m*/*z*): 873 (M^+ + 1H, 5%), 831 (M^+ − allyl, 7%), 709 (M^+ − 4allyl + 1H, 4%), 391 (NBA, 100%).

[Rh$_4$(μ-PyS$_2$)$_2$(CO)$_8$] (6). Carbon monoxide was bubbled through a solution of the complex [Rh$_4$(μ-PyS$_2$)$_2$(cod)$_4$] (**1**) (0.221 g, 0.196 mmol) in dichloromethane (10 mL) for 20 min. The color of the solution turned dark red, and then ethanol (15 mL) was added. The solvents were distilled under an atmosphere of carbon monoxide up to 4 mL to remove the displaced cyclooctadiene. Cooling of the solution at room temperature under a carbon monoxide atmosphere gave the complex as violet-black dichroic crystals, which were washed with cold ethanol and then dried under vacuum. Yield: 0.121 g (67%). Anal. Calcd for $C_{18}H_6N_2O_8Rh_4S_4$: C, 23.55; H, 0.66; N, 3.05. Found: C, 23.78; H, 0.85; N, 2.99. ^{1}H NMR ($CDCl_3$, 293 K): δ 7.37 (dd, 2H, H_m), 7.00 (dd, 2H, $H_{m'}$), 6.84 (dd, 2H, H_p) (J = 1.0 Hz, $J_{H_m-H_p}$ = 7.5 Hz, $J_{H_{m'}-H_p}$ = 8.1 Hz) (PyS_2 ligands). ^{13}C NMR ($CDCl_3$, 223 K): δ 184.3 (d, J_{RhC} = 64 Hz, CO), 182.2 (d, J_{RhC} = 73 Hz, CO), 182.0 (d, J_{RhC} = 72 Hz, CO), 181.6 (d, J_{RhC} = 64 Hz, CO), 168.6 (CS), 159.2 (CS), 136.9, 127.1, 123.0 (CH, Py). MS (FAB^+, toluene, *m*/*z*): 918 (M^+, 16%), 890 (M^+ − CO, 24%), 862 (M^+ − 2CO, 40%), 834 (M^+ − 3CO, 60%), 806 (M^+ − 4CO, 15%), 778 (M^+ − 5CO, 18%), 750 (M^+ − 6CO, 28%), 722 (M^+ − 7CO, 15%), 694 (M^+ − 8CO, 30%), 488 (M^+ − 2Rh − 8CO, 73%), 443 (Rh(CO)$_2$(PyS_2H)$_2$, 100%). IR (hexane, cm^{-1}): ν (CO), 2090 (m), 2072 (s), 2062 (s), 2024 (s), 2012 (m).

[Rh$_4$(μ-PyS$_2$)$_2$(CO)$_4$(PPh$_3$)$_4$] (7) was prepared from [{Rh(μ-Cl)(CO)(PPh_3)}$_2$] (0.250 g, 0.291 mmol), 2,6-dimercaptopyridine (0.041 g, 0.291 mmol), and *n*-BuLi (0.36 mL, 1.6 M in *n*-hexane, 0.583 mmol) in tetrahydrofuran (15 mL) following the method B described above for complex **1**. The dark red solution was concentrated under vacuum to *ca*. 1 mL, diethyl ether (5 mL) and methanol (10 mL) were slowly added, and the mixture was again concentrated. A red-violet solid crystallized out, which was washed repeatedly with cold methanol and then vacuum dried. Yield: 0.200 g (74%). Complex **7** can be alternatively synthesized by reaction of [Rh(acac)(CO)(PPh_3)] (0.075 g, 0.152 mmol) with Py(SH)$_2$ (0.022 g, 0.152 mmol) and NEt_3 (42 μL, 0.30 mmol, 0.73 g mL^{-1}) in dichloromethane (5 mL). Work-up as above gave **7** in 82% yield (0.058 g). Anal. Calcd for $C_{86}H_{66}N_2O_4P_4Rh_4S_4$: C, 55.68; H, 3.59; N, 1.51. Found: C, 55.37; H, 3.47; N, 1.63. ^{31}P NMR ($CDCl_3$, 218 K): δ 43.3 (d, J_{RhP} = 160 Hz), 41.5 (d, J_{RhP} = 167 Hz), 41.2 (d, J_{RhP} = 159 Hz), 40.1 (d, J_{RhP} = 166 Hz), 40.0 (d, J_{RhP} = 166 Hz), 39.6 (d, J_{RhP} = 167 Hz), 38.2 (d, J_{RhP} = 150 Hz), 37.5 (d, J_{RhP} = 167 Hz, mixture of isomers). MS (FAB^+, acetone, *m*/*z*):

Table 1. Summary of Crystal data for $[Rh_4(\mu\text{-}pyS_2)_2(cod)_4]$ (**1**)

formula	$C_{42}H_{54}N_2Rh_4S_4$	D_{calcd}, g cm^{-3}	1.881
mol wt	1126.8	λ (Mo K$_\alpha$) radiation, Å	0.710 73
cryst size, mm	0.086 × 0.137 × 0.315	temp, K	298
cryst syst	monoclinic	μ, mm^{-1}	1.874
space group	*C2/c* (No. 15)	transmn facts	0.636, 0.776
a, Å	10.252(1)	2θ range, deg	3−47
b, Å	17.023(2)	no. of data collctd	6381 (+*h*, ±*k*, ±*l*)
c, Å	23.114(3)	no. of unique data	2925 (R_{int} = 0.025)
β, deg	99.50(1)	unique obsd data	2393 [$(F_o) \geq 4\sigma(F_o)$]
V, Å^3	3978(1)	*R*, R_w[a]	0.0228, 0.0240
Z	4		

[a] $R = \sum[|F_o| - |F_c|]/\sum|F_o|$; $R_w = [\sum w(|F_o| - |F_c|)^2/\sum w|F_o|^2]^{1/2}$; $w^{-1} = \sigma^2(F_o) + 0.0001F_o^2$.

1855 (M^+, 80%), 1480 ($M^+ - 4CO - PPh_3$, 31%), 1218 ($M^+ - 4CO - 2PPh_3$, 35%), 391 (NBA, 100%). IR (CH_2Cl_2, cm^{-1}): ν(CO), 1975 (br, s).

[Rh$_2$(μ-PyS$_2$H)$_2$(cod)$_2$] (8). To a solution of [Rh(acac)(cod)] (0.150 g, 0.428 mmol) in dichloromethane (10 mL), solid 2,6-dimercaptopyridine (0.069 g, 0.482 mmol) was added to give a dark orange solution which was stirred for 30 min. Concentration of the solution resulted in partial precipitation of a solid which was completed by addition of a mixture of methanol−diethyl ether (1:1). The solid was isolated by filtration and washed with methanol. Complex **8** is obtained as an orange-brown solid by recrystallization from dichloromethane/methanol. Yield: 0.132 g (78%). Complex **8** can be alternatively synthesized by reaction of $Py(SH)_2$ (0.059 g, 0.410 mmol) with the solvated species $[Rh(cod)(Me_2CO)_x][BF_4]$ (0.410 mmol) prepared "in situ" by reaction of $[\{Rh(\mu\text{-}Cl)(cod)\}_2]$ (0.101 g, 0.205 mmol) with $AgBF_4$ (0.080 g, 0.410 mmol) in acetone. Work-up as described above gave **8** in 94% yield (0.136 g). Anal. Calcd for $C_{26}H_{32}N_2Rh_4S_4$: C, 44.19; H, 4.56; N, 3.96. Found: C, 43.66; H, 4.38; N, 4.00. MS (FAB$^+$, CH_2Cl_2, *m*/z): 916 (M^+ + Rh + cod, 41%), 706 (M^+, 37%), 598 (M^+ − cod, 29%), 564 ($M^+ - PyS_2$, 44%), 391 (NBA, 100%), 354 (M^+ − Rh − cod − PyS_2, 33%). MW ($CHCl_3$): calcd, 706; found, 873.

Synthesis of Heterotetranuclear Complexes. In a typical procedure [M(acac)(cod)] (0.300 mmol) (M = Rh, Ir) and 2,6-dimercaptopyridine (0.003 mmol) were reacted in dichloromethane (10 mL) for 15 min. Solid $[\{M'(\mu\text{-}OMe)(cod)\}_2]$ (M′ = Rh, Ir; M ≠ M′) was then added to give a purple-red solution. Concentration of the solution to *ca*. 1 mL and slow addition of methanol gave purple microcrystalline solids which were filtered, washed with methanol, and then vacuum dried. Characterization of the complexes was achieved by ^{1}H NMR and MS spectra (see text).

Crystal Structure Determination of [Rh$_4$(μ-PyS$_2$)$_2$(cod)$_4$] (1). Suitable crystals for the X-ray diffraction study were obtained by slow diffusion of methanol into a concentrated solution of **1** in a dichloromethane/diethyl ether mixture. The selected crystal was a red transparent irregular block of approximate dimensions 0.086 × 0.137 × 0.315 mm. Cell parameters were determined from 64 accurately centered reflections in the range 20 ≤ 2θ ≤ 47°. Intensity data were recorded using $\omega/2\theta$ scans (3 ≤ 2θ ≤ 47°) on a Siemens-Stoe AED-2 diffractometer equipped with a highly oriented graphite crystal monochromator. Crystal data and details associated with structure refinement are summarized in Table 1. Three standards reflections were monitored during data collection every 55 min of measuring time; crystal decay (≤1%) was corrected according the intensities of the standard reflections. Data were corrected for Lorentz and polarization effects, and a semiempirical correction, based on azimuthal ψ-scans from seven reflections, was also applied.[22]

The structure was solved by Patterson and Fourier methods. All non-hydrogen atoms were isotropically and subsequently anisotropically refined by full-matrix least-squares. All of the H-atoms were located and included in the final steps of refinement as free isotropic atoms. Residuals in the ΔF map were 0.35 e/Å^3. Scattering factors, corrected for anomalous dispersion, were taken from ref 23. All calculations were performed on a μ-VAX 3400 computer with the SHELXTL-PLUS package.[24] Final atomic coordinates and equivalent temperature factors are given in Table 2.

Table 2. Atomic Coordinates (×10^4; ×10^5 for Rh and S Atoms) and Equivalent Isotropic Displacement Coefficients[a] (Å^2, ×10^4) for the Complex $[Rh_4(\mu\text{-}pyS_2)_2(cod)_4]$ (**1**)

atom	*x*/*a*	*y*/*b*	*z*/*c*	U_{eq}
Rh(1)	22586(3)	95475(2)	13079(1)	293(1)
Rh(2)	−2713(3)	87364(2)	16403(1)	266(1)
S(1)	3713(11)	103524(7)	10510(5)	370(4)
S(2)	18082(10)	90630(6)	22256(4)	286(3)
N	−931(3)	9820(2)	1891(1)	254(11)
C(1)	−639(4)	10458(2)	1581(2)	290(13)
C(2)	−1149(5)	11194(3)	1694(2)	401(16)
C(3)	−1882(5)	11275(3)	2130(2)	443(17)
C(4)	−2111(5)	10636(3)	2464(2)	369(16)
C(5)	−1597(4)	9916(2)	2347(2)	259(13)
C(6)	2374(5)	9514(3)	383(2)	415(17)
C(7)	3088(5)	10157(3)	628(2)	408(17)
C(8)	4589(5)	10196(3)	765(2)	499(20)
C(9)	5120(5)	9970(3)	1385(2)	500(20)
C(10)	4302(5)	9356(3)	1618(2)	444(18)
C(11)	3766(5)	8684(3)	1329(2)	401(17)
C(12)	3994(7)	8422(4)	728(3)	545(22)
C(13)	2952(6)	8745(4)	240(2)	534(20)
C(14)	−2244(5)	8358(3)	1318(2)	408(17)
C(15)	−1743(5)	8741(3)	878(2)	406(16)
C(16)	−1221(7)	8342(3)	379(2)	531(20)
C(17)	−307(6)	7664(3)	572(2)	524(21)
C(18)	439(5)	7765(3)	1186(2)	396(17)
C(19)	21(5)	7502(3)	1681(2)	403(17)
C(20)	−1276(6)	7077(3)	1688(3)	511(20)
C(21)	−2445(6)	7485(3)	1352(3)	541(21)

[a] Equivalent isotropic *U* defined as one-third of the trace of the orthogonalized $\mathbf{U}_{ij}$ tensor.

Results and Discussion

Tautomerism of the Ligand. In the original preparations[20,21] of the ligand 2,6-dimercaptopyridine $[Py(SH)_2]$ the ^{1}H NMR spectrum was not described, probably because it is temperature and solvent dependent. At low temperature in toluene there is a single compound, the 3-mercapto-2(1*H*)-pyridinethione tautomer (A), in agreement with the ^{1}H NMR spectrum (see Experimental Section), which shows five well-defined resonances: three for the aromatic protons and two for the NH and SH protons. The two latter signals broaden as the temperature increases and become a broad band at room temperature which should be due to the acidic proton exchange. Further heating leads to broadening of the *meta* proton resonances, which eventually coalesce and became equivalent at high temperature. A reasonable explanation for the chemical equivalence of the *meta* protons is a shift to the right of the tautomeric equilibrium in Scheme 1 on raising the temperature. However, the ^{1}H and $^{13}C\{^1H\}$ spectra in $CDCl_3$ at room temperature are consistent with structure B (see Experimental Section). Obviously, the

(22) North, A. C. T.; Phillips, D. C.; Mathews, F. S. *Acta Crystallogr.* **1968**, *A24*, 351.
(23) *International Tables for X-Ray Crystallography*; Kynoch Press: Birmingham, England, 1974; Vol. 4.
(24) Sheldrick, G. M. SHELXTL PLUS Program for Crystal Structure Solution and Refinement; Siemens Analytical X-ray Instruments, Madison, WI, 1990.

Scheme 1

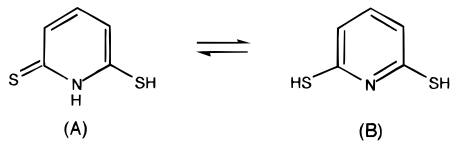

tautomeric equilibrium is influenced by the solvent, and polar solvents favor the shift to the more polar tautomer B.

Homotetranuclear Diolefin Complexes. Protonation of the methoxo groups in the dinuclear complexes [M(μ-OMe)(diolefin)]$_2$ (M = Rh, Ir) with binucleating ligands containing acidic protons is a convenient synthetic approach to dinuclear complexes, even if the pK_{MeOH} is smaller than pK_{ligand}.[25] In our case, the reaction of Py(SH)$_2$ with [{Rh(μ-OMe)(cod)}$_2$] (cod = 1,5-cyclooctadiene) in a molar ratio 1:1 gives the tetranuclear complex [Rh$_4$(μ-PyS$_2$)$_2$(cod)$_4$] (**1**), which is isolated as orange microcrystals in high yield (method A). Alternatively, the ligand Py(SH)$_2$ can be doubly deprotonated in situ by *n*-butyllithium in tetrahydrofuran to give a pale yellow solution. Further reaction of this solution with 1 equiv of [{Rh(μ-Cl)(cod)}$_2$] affords a mixture of **1** and lithium chloride, which is easily separated due to the insolubility of **1** in methanol (method B). This alternative synthetic route gives **1** in similar yield to that of route A but is less convenient since it requires the use of *n*-butyllithium.

Complex **1** is soluble in dichloromethane, tetrahydrofuran, and toluene, sparingly soluble in diethyl ether and hexanes, and insoluble in MeOH. Complex **1** was formulated as tetranuclear from mass spectroscopy, which shows the molecular ion at 1126 (M^+, 100%) with sequential loss of four 1,5-cyclooctadiene ligands. The IR spectrum shows three strong characteristic absorptions at 1560, 1540, and 1410 cm^{-1} due to the thioamide ν(C=N) + ν(S=C−N) modes[26] of 2,6-dimercaptopyridine, and the absence of both ν(SH) and ν(NH) absorptions in the IR confirms the presence of doubly deprotonated ligands in the complex.

The related diolefin rhodium complexes, [Rh$_4$(μ-PyS$_2$)$_2$(nbd)$_4$] (**2**) and [Rh$_4$(μ-PyS$_2$)$_2$(tfbb)$_4$] (**3**) (nbd = norborna-2,5-diene, tfbb = tetrafluorobenzo[5,6]bicyclo[2.2.2]octa-2,5,7-triene), have been also prepared following the methods described for **1**. Complex **2** is isolated as a red-purple solid insoluble in the usual organic solvents, while complex **3** is a dark red solid with greater solubility which enabled its characterization by mass and NMR spectroscopies. Both show the characteristic strong thioamide absorptions in their IR spectra at 1560, 1540, and 1410 cm^{-1}, probably associated with the coordination mode of the PyS$_2^{2-}$ ligand in the tetranuclear framework.

Other tetranuclear complexes of different metals can be prepared by the above described routes. So, the iridium(I) and palladium(II) complexes [Ir$_4$(μ-PyS$_2$)$_2$(cod)$_4$] (**4**) and [Pd$_4$(μ-PyS$_2$)$_2$(allyl)$_4$] (**5**) result from the reaction of the corresponding chloro complexes [{M(μ-Cl)L$_2$}$_2$] (M = Ir, L$_2$ = cod; M = Pd, L$_2$ = allyl) with a solution of Li$_2$PyS$_2$ prepared in situ. They are isolated in high yield as black-red and orange microcrystalline solids, respectively. Complex **4** is also accessible by direct protonation of the methoxo ligands in [{Ir(μ-OMe)(cod)}$_2$]. The tetranuclear formulation of complexes **4** and **5** is confirmed by their mass spectra, which show the molecular ions at the expected values of *m*/*z*.

In order to establish the coordination of the bridging ligands and to obtain accurate geometrical parameters to elucidate the fluxional behavior of the tetranuclear complexes, a single crystal X-ray analysis of complex **1** was carried out. Figure 1 shows a representation of the molecule together with the atom labeling scheme used. Table 3 displays selected bond distances and angles.

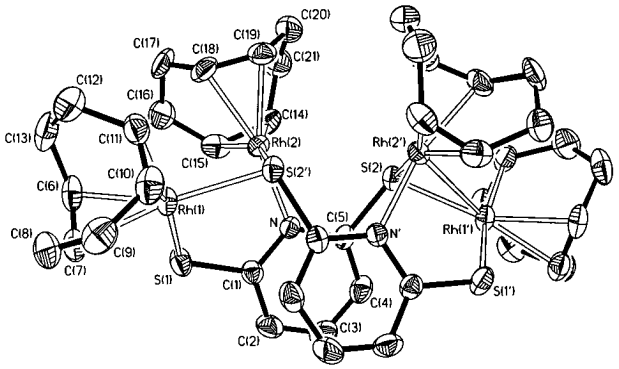

Figure 1. View of the molecular structure of [Rh$_4$(μ-PyS$_2$)$_2$(cod)$_4$] (**1**) showing the atom labeling scheme. Hydrogen atoms have been labeled with the number of the carbon to which they are bonded.

Table 3. Selected Bond Lengths (Å) and Angles[a] (deg) for [Rh$_4$(μ-pyS$_2$)$_2$(cod)$_4$]

Rh(1)···Rh(2)	3.1435(5	Rh(2)···Rh(2′)	3.9210(6)
Rh(1)−S(1)	2.365(1)	Rh(2)−N	2.080(3)
Rh(1)−S(2′)	2.391(1)	Rh(2)−S(2)	2.394(1)
Rh(1)−C(6)	2.161(4)	Rh(2)−C(14)	2.136(5)
Rh(1)−C(7)	2.171(5)	Rh(2)−C(15)	2.123(4)
Rh(1)−C(10)	2.125(5)	Rh(2)−C(18)	2.149(5)
Rh(1)−C(11)	2.128(5)	Rh(2)−C(19)	2.122(4)
C(6)−C(7)	1.383(7)	C(14)−C(15)	1.378(7)
C(10)−C(11)	1.392(7)	C(18)−C(19)	1.361(7)
S(1)−C(1)	1.739(4)	S(2)−C(5)	1.789(4)
N−C(1)	1.362(5)	N−C(5)	1.356(5)
C(1)−C(2)	1.398(6)	C(4)−C(5)	1.378(6)
C(2)−C(3)	1.361(7)	C(3)−C(4)	1.375(7)

S(1)−Rh(1)−S(2′)	98.79(4)	N−Rh(2)−S(2)	86.4(1)
S(1)−Rh(1)−M(1)	86.6(1)	N−Rh(2)−M(3)	91.2(1)
S(1)−Rh(1)−M(2)	170.0(1)	N−Rh(2)−M(4)	174.4(1)
S(2′)−Rh(1)−M(1)	173.3(1)	S(2)−Rh(2)−M(3)	174.5(1)
S(2′)−Rh(1)−M(2)	88.8(1)	S(2)−Rh(2)−M(4)	96.4(1)
M(1)−Rh(1)−M(2)	86.4(1)	M(3)−Rh(2)−M(4)	86.4(1)
Rh(1)−S(1)−C(1)	116.1(1)	Rh(1)−S(2′)−Rh(2)	82.13(3)
S(1)−C(1)−N	119.8(3)	Rh(1)−S(2′)−C(5′)	105.6(1)
S(1)−C(1)−C(2)	120.6(3)	Rh(2)−S(2′)−C(5′)	108.8(1)
N−C(1)−C(2)	119.6(4)	Rh(2)−N−C(1)	116.7(2)
S(2)−C(5)−N	117.0(3)	Rh(2)−N−C(5)	123.5(2)
S(2)−C(5)−C(4)	121.9(3)	C(1)−N−C(5)	119.7(3)
N−C(5)−C(4)	121.1(3)		

[a] Primed atoms are related to the unprimed ones by the symmetry transformation $-x$, y, $^1/_2 - z$. M(1), M(2), M(3) and M(4) are the midpoints of the olefinic bonds C(6)−C(7), C(10)−C(11), C(14)−C(15), and C(18)−C(19), respectively.

The crystal structure of **1** consists of tetranuclear complexes packed with no close intermolecular contacts. The molecule exhibits a crystallographically imposed C_2 symmetry with only one independent "Rh$_2$(μ-PyS$_2$)(cod)$_2$" moiety in the asymmetric unit. The two related 2,6-pyridinedithiolate groups bridge all of the four metal centers acting as tridentate ligands; they are bonded through the pyridinic nitrogen and through both sulfur atoms with one of them coordinated in a μ_2 fashion to two different metal centers. Each rhodium has a slightly distorted square-planar environment with a chelating cyclooctadiene molecule interacting through the two olefinic bonds. The shortest intermetallic separation, Rh(1)···Rh(2), is 3.1435(5) Å and excludes any but the weakest interaction between the metals; the Rh(2)···Rh(2′) distance across the C_2 axis is significantly longer, 3.9210(6) Å.

(25) (a) Ciriano, M. A.; Pérez-Torrente, J. J.; Oro, L. A. *J. Organomet. Chem.* **1993**, *445*, 267. (b) Oro, L. A.; Fernandez, M. J.; Modrego, J.; López, J. M. *J. Organomet. Chem.* **1985**, *287*, 409.
(26) Raper, E. S. *Coord. Chem. Rev.* **1985**, *61*, 115.

The 2,6-pyridinedithiolate bridging ligand is roughly planar. The sulfur atoms display deviations from the pyridinic ring of 0.144(1) and 0.104(1) Å for S(1) and S(2), respectively. The dihedral angle between the two symmetry related dithiolate ligand planes is 26.7(1)°. If compared with the related 2-mercaptopyridine free base,[27] the most remarkable feature is the elongation of the C−S bond distances from 1.692(2) Å, in the free related ligand, to 1.739(4) (C(1)−S(1)) and 1.789(4) Å (C(5)−S(2)). These changes clearly evidence that one of the C−S bonds maintain a clear thione character, as a consequence of the electronic donation upon coordination to the metal. As expected, the C(5)−S(2) distance is longer than C(1)−S(1), corresponding with the μ_2 character of the S(2) atom. However, both C−S distances are significantly shorter than typical C−S single bonds, for instance, 1.829(26) Å in alkanethiolates,[28] showing the partial aromaticity of the bridging ligands.

The Rh−S bond distances (2.365(1) Å for Rh(1)−S(1), the slightly longer distances for the bridging S(2) atom (2.391(1) and 2.394(1) Å), and the Rh−N length (2.080(3) Å) compare well with complexes containing the closely related N−S donor ligands as benzothiazole-2-thiolate or pyridine-2-thiolate (mean values 2.38(8) Å for Rh−S and 2.13(7) Å for Rh−N).[29] The square-planar metal environments are slightly distorted and exhibit deviations always under 0.215(4) Å. Both independent metal coordination planes are almost perpendicular making a dihedral angle of 97.0(1)°.

Each cyclooctadiene ring has a boat conformation with a mean carbon−carbon double bond length of 1.379(6) Å. Interestingly, within the accuracy obtained, the asymmetry observed in the other side of the metal coordination spheres does not affect significatively the coordination of the diolefinic molecules; only the Rh(1)−C bond distances *trans* to the S(2′) are slightly longer than the rest.

NMR Studies on the Diolefin Complexes. The diolefin complexes **1**, **3**, and **4** behave in a similar way, judging from their ^{1}H and ^{13}C NMR spectra. They show equivalent and apparently static bridging ligands, while there is a fluxional movement associated with the diolefin groups. This nonrigidity in a polynuclear complex was intriguing and was investigated further.

Figure 2 shows the variable temperature ^{1}H NMR spectra of the diolefinic region for complex **4** as a representative example. Eight well-defined olefinic proton resonances are observed for the complexes at low temperature. In addition, their ^{13}C{^{1}H} NMR spectra show also eight resonances for the olefinic carbons in the slow-exchange region. Moreover, the resonances for the C−S carbons of the pyridine ring appear in the ^{13}C{^{1}H} NMR spectra as two different singlets as a consequence of the coordination mode of the bridging ligand. These data are in accordance with the structure found in the solid state for **1**, where there are two types of equivalent diolefin ligands, the inner and the external. In addition, molecular weight determinations for complexes **1**, **3**, and **4** confirm that the species in solution are tetranuclear. Hence, all the olefinic complexes are concluded to have the structure found for complex **1** in solution. The C_2 symmetry of the tetranuclear structure let us simplify the discussion by treating the complexes as dinuclear having the A-frame structure of half of the molecule, *i.e.* two different bridges and hence lacking any element of symmetry.

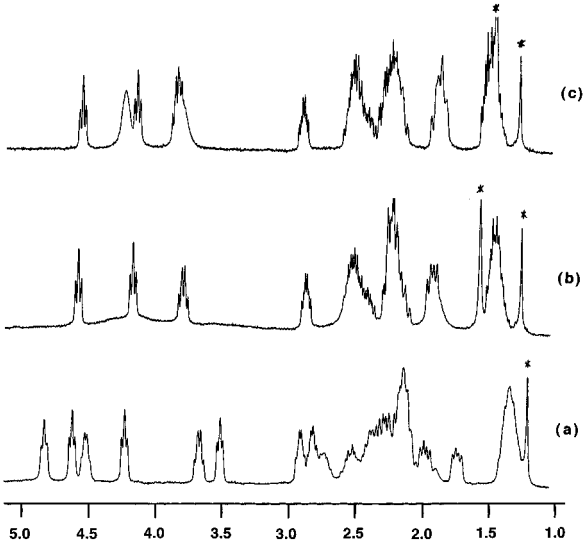

Figure 2. Variable temperature spectrum of [$Ir_4(\mu$-$PyS_2)_2(cod)_4$] (**4**) at (a) 223, (b) 293, and (c) 328 K in $CDCl_3$. The water and pentane peaks are denoted by asterisks.

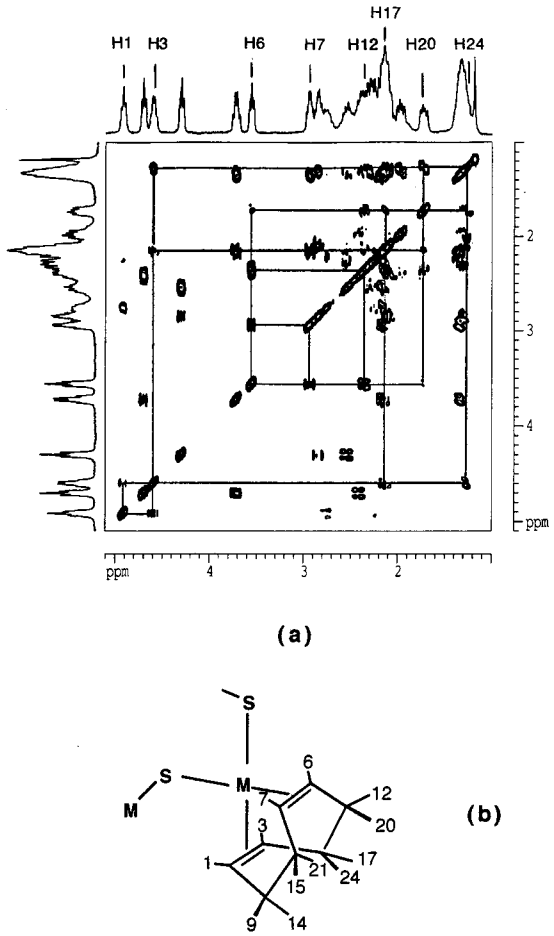

Figure 3. (a) H,H-COSY spectrum of the diolefin region of [$Ir_4(\mu$-$PyS_2)_2(cod)_4$] (**4**) at the slow-exchange region and (b) map of the "mobile" diolefin.

The H,H-COSY spectra at low temperature allow the identification of the four pairs of resonances related by coupling, *i.e.*, those of the protons bonded to a given C═C bond. Namely, they are those at δ 4.95 and 4.60, 4.70 and 3.75, 4.30 and 2.85, and 3.60 and 2.95 for complex **4** (Figure 3a). Further information for assigning the resonances from each diolefin was obtained from the variable temperature spectra, since they show that one type of the diolefin ligands is rigid whereas the other

(27) Ohms, U.; Guth, H.; Kutoglu, A.; Scheringer, C. *Acta Crystallogr.* **1982**, *B38*, 831.
(28) Orpen, A. G.; Brammer, L.; Allen, F. H.; Kennard, O.; Watson, D. G.; Taylor, R. *J. Chem. Soc., Dalton Trans.* **1991**, S1.
(29) Ciriano, M. A.; Pérez-Torrente, J. J.; Lahoz, F. J.; Oro, L. A. *J. Organomet. Chem.* **1993**, *455*, 225.

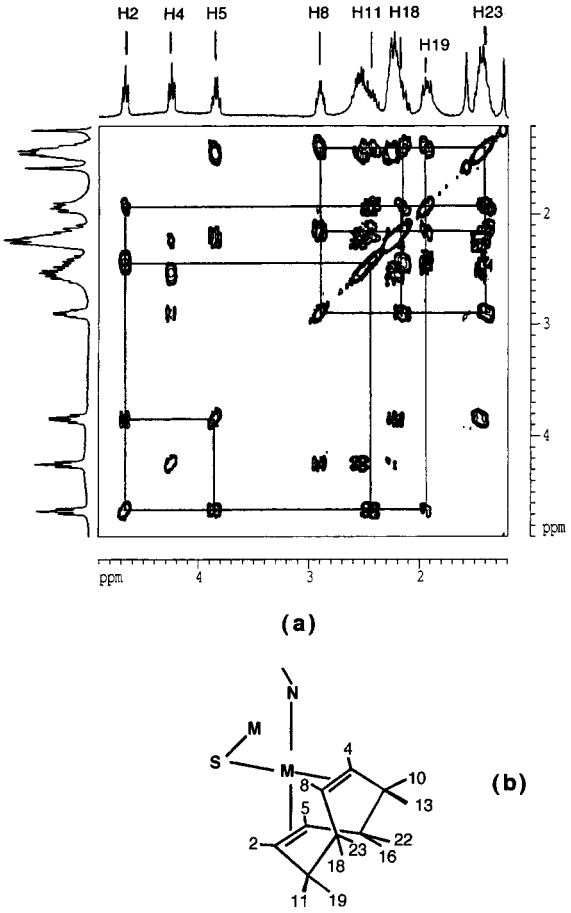

Figure 4. (a) H,H-COSY spectrum of the diolefin region of $[Ir_4(\mu\text{-}PyS_2)_2(cod)_4]$ (**4**) nearly at the coalescence temperature and (b) map of the static diolefin ligand.

undergoes a fluxional motion. Figure 2b corresponds to the spectrum of **4** at the temperature of coalescence, showing that the resonances at δ 4.70 (H(2)) and 3.75 (H(5)), 4.30 (H(4)) and 2.85 (H(8)) are due to the rigid diolefin. Furthermore, the H,H-COSY spectrum at this temperature (Figure 4a) allows the construction of the map of this diolefin as shown in Figure 4b. Therefore, H(2) is coupled with the olefinic H(5) and with the methylene exo and endo protons H(11) and H(19); H(19) is also coupled to H(18) and H(23), which, in turn, are coupled to the olefinic H(8). In a similar way, the relationships between the protons of the diolefin to complete the cycle can be easily located in this COSY spectrum. The maps of the rigid and "mobile" diolefins can be calculated in a similar way from the low-temperature COSY spectrum (Figure 3a). Therein are depicted the relationships between the protons of a half of the cycle of the mobile diolefin by example. Therefore, H(6) is coupled with the olefinic H(7) and with the methylene exo and endo protons H(12) and H(20); H(20) is also coupled to H(17) and H(24), which, in turn, are coupled to the olefinic H(3). The map of this diolefin is in Figure 3b.

Once the two sets of resonances due to the two distinct diolefin ligands have been identified, two problems arise: firstly, the decision of which diolefin is which and secondly the assignment of the olefin signals within each. To address these points, another technique independent of the chemical shift should be desirable such as the nuclear Overhauser effect (NOE) previously used for structural purposes. Nevertheless, the olefinic protons are far away from those of the bridging ligands, and NOE effects between them should not be observable. On the other hand, a careful observation of the structure of **1** in the solid state allows the detection of a close proximity (2.57 Å) between two olefinic protons, one from each diolefin ligand, namely, those bonded to C(11) and C(18) in Figure 1. Identification of these resonances by NOE experiments would allow the full assignment of the diolefinic protons. Unfortunately NOESY experiments on complex **4** are not conclusive since chemical exchange still occurs at 225 K and the assignments need to be done on the basis of the chemical intuition. Closer inspection of the crystal structure reveals a difference between both types of ligands. The inner diolefin is *trans* to the nitrogen and a bridging sulfur, while the outer olefin is *trans* to a bridging and to a terminal sulfur. In our experience with complexes containing bridging N−C−S ligands, the presence of free lonely pairs on the sulfur donor atom give rise to fluxionality[12e] due to the well-known inversion at the sulfur,[30] while static NMR are shown by either complexes with a metal−metal bond[12a] or trinuclear complexes where all the donor electron pairs of the bridging ligand are involved in coordination.[13a,b] On this basis, the rigid diolefin should be the inner one, where the lone pairs of the *trans* sulfur are engaged.

To assign the protons of the rigid diolefin, it should be noted that those resonances at lower field (H(2) and H(5)) correspond to the olefinic bond *trans* to the nitrogen, as pointed out by Mann[31] for open-book dinuclear 2-pyridonate iridium complexes. Therefore, H(4) and H(8) are *trans* to the bridging sulfur atom. Furthermore, for the mobile diolefin H(1) and H(3) should be *trans* to the terminal sulfur atom and, hence, H(6) and H(7) *trans* to the bridging sulfur. No further assignment can be made on the basis of the data available, but it is remarkable that the chemical shift of the olefin resonances is influenced in the same amount both by their relative position in the molecule, being inside or outside of the A-frame, and by the atom *trans* to them.

Inspection of the ^1H and $^{13}C\{^1H\}$ NMR spectra of **4** at high temperature reveals that two pairs of the olefinic protons and carbons of the outer diolefin became equivalent in the fast exchange region. Moreover, these signals result from two different C═C bonds, and the NOESY spectrum of **4** confirms that the interchanging protons are H(1) with H(6) and H(3) with H(7), *i.e.*, those related by a rotation of the diolefin ligand around an axis passing through the metal, coincident with the bisectrix of the S−M−S angle. As the $^{13}C\{H\}$ NMR spectrum shows, the pyridine CS resonances are unaffected and well-differentiated. No change in the coordination of the bridging ligands occurs, and hence, the motion of the diolefin can be described as a rotation assisted by the inversion at the sulfur. The energy of activation for this motion can be estimated in 12 kcal/mol using the DNMR6 program,[32] a value expected for the rotation of olefin ligands.[33]

On the other hand, the tetranuclear palladium complex **5** exists in solution as a mixture of isomers, as deduced from its ^1H NMR spectrum, and was not investigated further.

Homotetranuclear Rhodium Carbonyl Complexes. Complex $[Rh_4(\mu\text{-}PyS_2)_2(CO)_8]$ (**6**) is obtained by carbonylation of **1** in dichloromethane at atmospheric pressure. The carbonylation process is partially reversible since when freshly made solutions of complex **6** are concentrated under vacuum in the presence of cyclooctadiene, the isolated black residue shows the molecular ion for the species $[Rh_4(\mu\text{-}PyS_2)_2(CO)_6(cod)]$ (m/z = 971).

(30) Abel, E. W.; Orrell, K. G.; Bhargava, S. K. *Prog. Inorg. Chem.* **1984**, *32*, 1.
(31) Rodman, G. S.; Mann, K. R. *Inorg. Chem.* **1988**, *27*, 338.
(32) Brown, J. H.; Bushweller, C. H. *DNMR6: Calculation of NMR Spectra (I = 1/2) Subject to the Effects of Chemical Exchange*; QCPE Program No. 633; Indiana University: Bloomington, IN.
(33) Vierkötter, S. A.; Barnes, C. E.; Garner, G. L.; Butler, L. G. *J. Am. Chem. Soc.* **1994**, *166*, 7445.

Isolation of pure complex **6** requires the removal of the replaced cyclooctadiene by distillation with ethanol. Alternative routes to **6** give poorer results. For example, the reaction of Li_2PyS_2 and $[\{Rh(\mu\text{-}Cl)(CO)_2\}_2]$ in tetrahydrofuran or toluene gives pyrophoric black-green solids.

Complex **6** is isolated as dark-violet dichroic crystals which turn into a green solid when pulverized. Solutions of **6** in any solvent are intensively colored and exhibit red-green dichroism. The tetranuclear framework of **1** is maintained on carbonylation. So, the mass spectrum shows the molecular ion at $m/z = 918$ with sequential loss of eight carbonyl ligands. In addition, the $^{13}C\{^1H\}$ NMR spectrum at low temperature shows equivalent bridging ligands and four doublets for the carbonyl groups due to coupling to the rhodium-103 active nuclei in accordance with a structure similar to that found for **1** but with carbonyl groups as ancillary ligands. The presence of bridging and terminal S-donor atoms is determined by two distinctive resonances for the C(S) atoms of the 2,6-pyridinedithiolate ligands, as observed in the $^{13}C\{^1H\}$ spectra of complex **1**. On warming, two of the carbonyl doublets collapse and a new doublet emerges at the midway point so that the two carbonyl ligands became equivalent. This effect should be attributed again to the inversion at the sulfur atoms coordinated to the external rhodium dicarbonyl groups.

Freshly made solutions of complex **6**, prepared by reaction of **1** with carbon monoxide in dichloromethane, react with 4 equiv of triphenylphosphine to give solutions that contain $[Rh_4(\mu\text{-}PyS_2)_2(CO)_4(PPh_3)_4]$ (**7**) and other unidentified Rh(I) species. Complex **7** is obtained pure in high yield as a red-purple solid by reaction of *trans*-$[Rh(\mu\text{-}Cl)(CO)(PPh_3)]_2$ with Li_2PyS_2 in tetrahydrofuran. The IR spectrum of **7** in dichloromethane shows a broad absorption at 1975 cm^{-1}, suggesting that each rhodium atom contains a carbonyl and a triphenylphosphine ligand; otherwise the presence of the "*cis*-$Rh(CO)_2$" units should be detected.[34] The $^{31}P\{^1H\}$ NMR spectrum at room temperature consists of a broad doublet on a background of broad resonances ranging from 43 to 35 ppm. When the spectrum is recorded at 223 K (Figure 5a), doublets from a mixture of different species are observed. Bearing in mind the framework of complex **1**, a large number of isomers are possible from the relative disposition of the CO and PPh_3 ligands on each rhodium center. Nevertheless, replacement of carbonyl ligands by triphenylphosphine in related tetracarbonyl dinuclear rhodium complexes having N and S donor atoms occurs *trans* to the sulfur; for example in $[Rh_2(\mu\text{-bzta})_2(CO)_3(PPh_3)]$ (bzta: benzothiazole-2-thiolate) and $[\{Rh(\mu\text{-bzta})(CO)(PPh_3)\}_2]$.[29] In a similar way, replacement of the carbonyl ligands in the assymmetric bridged binuclear complex $[Rh_2(\mu\text{-pz})(\mu\text{-S}^t\text{Bu})(CO)_4]$ occurs exclusively *trans* to the thiolate ligand.[35] Taking this into consideration, the triphenylphosphine ligands should be *trans* to the sulfur atoms in the two inner rhodium atoms coordinated both to N and S. Therefore, the observed mixture should be made from isomers having different relative dispositions of both carbonyl and triphenylphosphine ligands on the external rhodium atoms. Figure 5b shows the three possible isomers resulting from this consideration. Interpretation of the $^{31}P\{^1H\}$ NMR spectrum is now straightforward: the low-field doublet resonances at 43.3 and 41.5 ppm are assigned to a C_2 isomer (●), where two sets of equivalent phosphine ligands are expected; the high-field doublets at 38.2 and 37.5 ppm are attributed to the other C_2 isomer (*), and finally, the resonances at 41.2, 40.1, 40.0, and 39.6 ppm correspond to the C_1 isomer. The observed coupling constants ($^1J_{RhP}$) around 160 Hz are in accordance with triphenylphosphine ligands trans to S-donor atoms.[36]

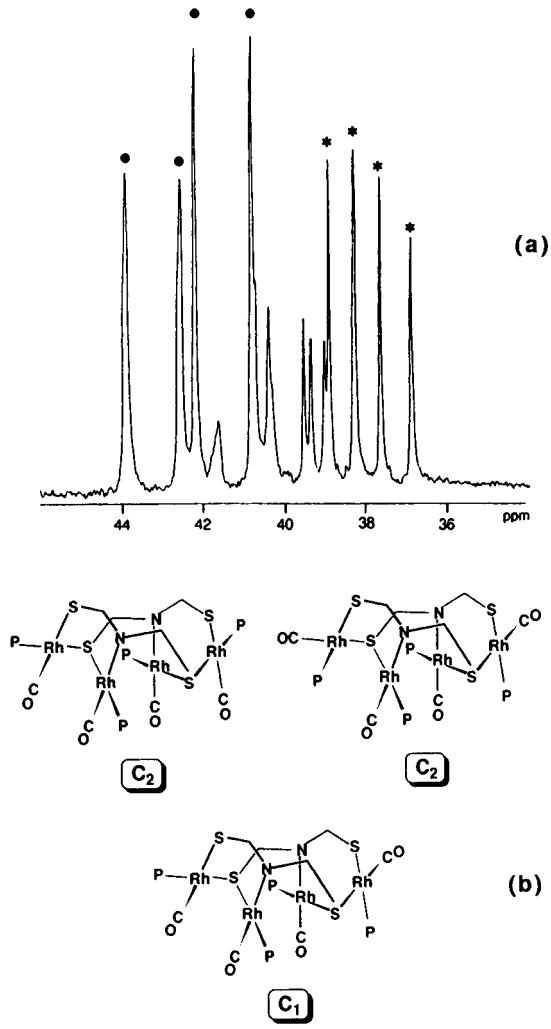

Figure 5. $^{31}P\{^1H\}$ NMR spectrum of $[Rh_4(\mu\text{-}PyS_2)_2(CO)_4(PPh_3)_4]$ (**7**) at 223 K (a) with the assignation to the isomers (b).

Approach to the Synthesis of Heterotetranuclear Complexes. Protonation of acetylacetonate complexes [M(acac)(diolefin)] or methoxide bridged complexes $[\{M(\mu\text{-OMe})(diolefin)\}_2]$ with binucleating ligands containing acidic protons give similar results for the synthesis of binuclear rhodium(I) or iridium(I) complexes,[37] although sometimes unexpected compounds have been prepared following the "acac route".[38] The protonation of [Rh(acac)(cod)] with $Py(SH)_2$ can be carried out stepwise. Using a molar ratio of 1:1, the dinuclear complex $[Rh_2(\mu\text{-}PyS_2H)_2(cod)_2]$ (**8**) is isolated, while in a molar ratio of 2:1 a tetranuclear aggregate $[Rh_4(\mu\text{-}PyS_2)_2(cod)_4]$ (**1**) is obtained (method C, Experimental Section). A small amount of **1** is also formed in the synthesis of **8**, which is easily removed by recrystallization. Complex **8** can be alternatively prepared by reaction of 2,6-dimercaptopyridine with the solvated species

(34) (a) Bruce, M. I.; Goodall, B. L.; Iqbal, M. Z., Stone, F. G. A. *J. Chem. Soc., Chem. Commun.* **1971**, 661. (b) Khan, Md. N. I.; Fackler, J. P., Jr.; King, C.; Wang, S. *Inorg. Chem.* **1988**, *27*, 1672.

(35) Claver, C.; Kalck, P.; Ridmy, M.; Thorez, A.; Oro, L. A.; Pinillos, M. T.; Apreda, M. C.; Cano, F. H.; Foces-Foces, C. *J. Chem. Soc., Dalton Trans.* **1988**, 1523.

(36) Osakada, K.; Matsumoto, K.; Yamamoto, A. *Organometallics* **1985**, *4*, 857.

(37) (a) Oro, L. A.; Pinillos, M. T.; Tejel, C.; Apreda, M. C.; Foces-Foces, C.; Cano, F. H. *J. Chem. Soc., Dalton Trans.* **1988**, 1927. (b) Oro, L. A.; Pinillos, M. T.; Tejel, C.; Foces-Foces, C.; Cano, F. H. *J. Chem. Soc., Dalton Trans.* **1986**, 1087.

(38) (a) Calvo, M. A.; Manotti-Lanfredi, A. M.; Oro, L. A.; Pinillos, M. T.; Tejel, C.; Tiripicchio, A.; Ugozzoli, F. *Inorg. Chem.* **1993**, *32*, 1147. (b) Oro, L. A.; Ciriano, M. A.; Villarroya, B. E.; Tiripicchio, A.; Lahoz, F. J. *J. Chem. Soc., Chem. Commun.* **1984**, 521.

Scheme 2. Synthetic Methods for $[Rh_4(\mu\text{-}PyS_2)_2(cod)_4]$ and $[Rh_2(\mu\text{-}PyS_2H)_2(cod)_2]$

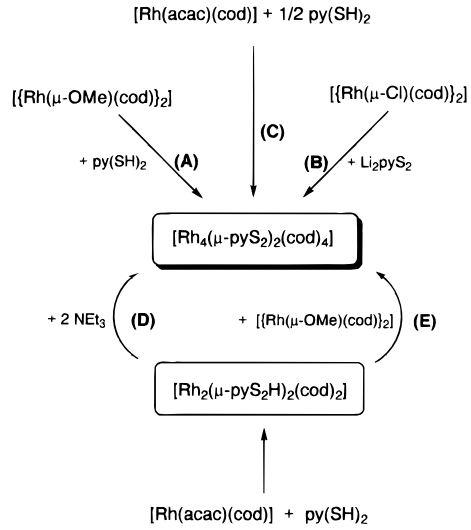

$[Rh(cod)(Me_2CO)_x][BF_4]$ in acetone. HBF_4 is thus produced in the reaction upon binding of the $Py(SH)_2$ ligands to rhodium (Scheme 2).

Characterization of **8** as dinuclear is based upon analytical results. Its mass spectrum shows the molecular ion at the expected $m/z = 706$ (37%), but also the trinuclear aggregate $[Rh_3(PyS_2H)_2(cod)_3]^+$ ($m/z = 916$, 12%) is detected. Complex **8** is a nonconductor in dichloromethane, and its molecular weight in chloroform is invariantly higher than the expected, suggesting an associative process in solution. In fact, the ^1H NMR spectrum shows a mixture of two species containing PyS_2H^- ligands, showing resonances at 13.00 and 12.37 ppm assignable to NH and a signal at 5.56 ppm for the SH protons. The broad resonances at 12.37, 6.91, 4.30, 2.46, and 1.95 ppm correspond to the main component which is fluxional. The minor species has inequivalent PyS_2H^- ligands which display six resonances at 7.45 (d), 7.30 (d), 6.90 (m), 6.65 (m), and 6.55 ppm; the cyclooctadiene resonances are shown as multiplets widespread between 5.1 and 1.5 ppm. In agreement with the spectroscopic information the structural proposals are adventurous in view of the possible coordination modes of the PyS_2H^- ligands. In spite of the fact that complex $[Rh_2(\mu\text{-}PyS_2H)_2(cod)_2]$ (**8**) exists as a mixture in solution, it behaves as the precursor of the tetranuclear aggregate **1** (Scheme 2) by deprotonation with 2 equiv of NEt_3 (method D). Interestingly, deprotonation of the bridging ligands can be accomplished by methoxo bridged dinuclear complexes. Therefore, a solution of **8** reacts with 1 equiv of $[\{Rh(\mu\text{-}OMe)(cod)\}_2]$ to give **1** in high yield (method E).

This synthetic approach could be explored to build heterotetranuclear complexes since it allows the construction of the tetranuclear framework in two steps. If appropriate starting materials containing different metals are used (M and M′), tetranuclear complexes having a heterometallic core $[M_2M_2']$ could be prepared. Hence, when [Rh(acac)(cod)] is reacted with 1 equiv of $Py(SH)_2$ and then with a half-equivalent of the dinuclear complex $[\{Ir(\mu\text{-}OMe)(cod)\}_2]$, a dark purple microcrystalline solid is obtained. The mass spectrum shows a peak for the expected heterotetranuclear core $[Rh_2Ir_2]$ at $m/z = 1306$ but also peaks at $m/z = 1396$, 1218, and 1126, corresponding to the cores $[RhIr_3]$, $[Rh_3Ir]$, and $[Rh_4]$, respectively, are observed. In order to elucidate if the observed distribution of products arise from recombination of produced fragments in the MS spectrum, a careful inspection of the ^1H NMR is necessary. The aromatic region shows multiple doublets for the most deshielded *meta* protons of the aromatic ring; the number of observed resonances is greater than that expected for the $[Rh_2Ir_2]$ aggregate, even if the four possible isomers are accounted for. So, the lack of selectivity in the synthesis of the heterotetranuclear aggregates is a direct consequence of the way of formation and probably of the nature of the binuclear precursor **8**. Attempts to obtain separate fractions with identical metal core by recrysallization were unsuccessful.

In a parallel manner, when [Ir(acac)(cod)] is reacted with 1 equiv of $Py(SH)_2$ and then with a half-equivalent of $[\{Rh(\mu\text{-}OMe)(cod)\}_2]$, solid samples containing heterotetranuclear aggregates with cores $[Rh_2Ir_2]$, $[RhIr_3]$, and $[Rh_3Ir]$, but no $[Ir_4]$, are obtained. Monitoring the reaction by ^1H NMR shows some degree of selectivity at the first stages since four doublets, for the *meta* protons are dominant over the others. Nevertheless, a distribution of products similar to that found in the above experiment is observed when the reaction time is increased to 24 h, suggesting that an intermolecular rearrangement of the tetranuclear frameworks formed at the beginning of the reaction occurs.

Electrochemical Studies. The cyclic voltammetry of $[Rh_4(\mu\text{-}PyS_2)_2(cod)_4]$ (**1**) in dichloromethane shows three successive anodic processes at peaks A−C (Figure 6a). The analysis[39,40] of the waves A/E and B/D with scan rates varying from 0.05 to 0.20 V s^{-1} indicates that they are reversible one-electron oxidations.[41] The third anodic response (peak C) at 1.21 V (at 0.1 V s^{-1}) shows typical features of an irreversible electron transfer.[40] The response of complex **1** at the RDE confirms that the two first steps at the formal electrode potentials $E_{1/2} = 0.16$ V and $E_{1/2} = 0.58$ V, corresponding to the waves A/E and B/D, are one-electron oxidations, which is in accordance with the formation of the mono-$[Rh_4(\mu\text{-}PyS_2)_2(cod)_4]^+$ and dicationic $[Rh_4(\mu\text{-}PyS_2)_2(cod)_4]^{2+}$ species having the cores $[Rh_4]^{5+}$ ($Z = +1$) and $[Rh_4]^{6+}$ ($Z = +2$), respectively. The third step, corresponding to the anodic process C, has a double limiting current per concentration unit relative to the other two. Therefore, the anodic response C probably involves a two-electron process. The electrochemical behavior for the related complex $[Rh_4(\mu\text{-}PyS_2)_2(tfbb)_4]$ (**3**) in dichloromethane is quite similar to that found for **1**. Two reversible one-electron oxidations are observed at formal electrode potentials ($E_{1/2}$) 0.37 and 0.79 V. Interestingly, both are shifted 210 mV to higher potential relative to those observed for **1**.

Complex $[Rh_4(\mu\text{-}PyS_2)_2(CO)_8]$ (**6**) shows irreversible oxidations at −0.05, +0.62, and +1.21 V (at 0.1 V s^{-1}). The wave up to the solvent anodic limit gives poorly defined voltammetric pictures because of the coalescence of several oxidation steps. When the scan is reversed, two broad irreversible reduction peaks at +0.2 and −1.38 V (at 0.1 V s^{-1}) are observed. Analysis of the cathodic response indicates that both reduction

(39) Brown, E. R.; Sandifer, J. R. In *Physical Methods of Chemistry: Electrochemical Methods*; Rossiter, B. W., Hamilton, J. F., Eds.; Wiley: New York, 1986; Vol. 2.

(40) Analysis of waves A/E and B/D shows values of $i_{p(E)}/i_{p(A)}$ and $i_{p(D)}/i_{p(B)}$ ratios equal to 1 at any scan rate; the $i_{p(A)}\upsilon^{-1/2}$ and $i_{p(B)}\upsilon^{-1/2}$ current functions are constant, and the differences $[E_{p(A)} - E_{p(E)}]$ and $[E_{p(B)} - E_{p(D)}]$ are constantly equal to 63 and 72 mV, respectively. The ΔE_p term departure from the theoretical value of 59 mV is rather common when dichloromethane is used as solvent (Mabbott, G. A. *J. Chem. Educ.* **1983**, *60*, 697). Analysis of peak C with scan rates varying from 0.01 to 1 V s^{-1} shows no reduction peak associated with C. In addition, the current function $i_{p(C)}{}^{-1/2}$ is approximately constant, indicating that the process is diffusion-controlled and the value of the potential $E_{p(C)}$ increases by 70 mV for a 10-fold increase in *V*.

(41) Piraino, P.; Bruno, G.; Tresoldi, G.; Lo Schiavo, S.; Zanello, P. *Inorg. Chem.* **1987**, *26*, 91.

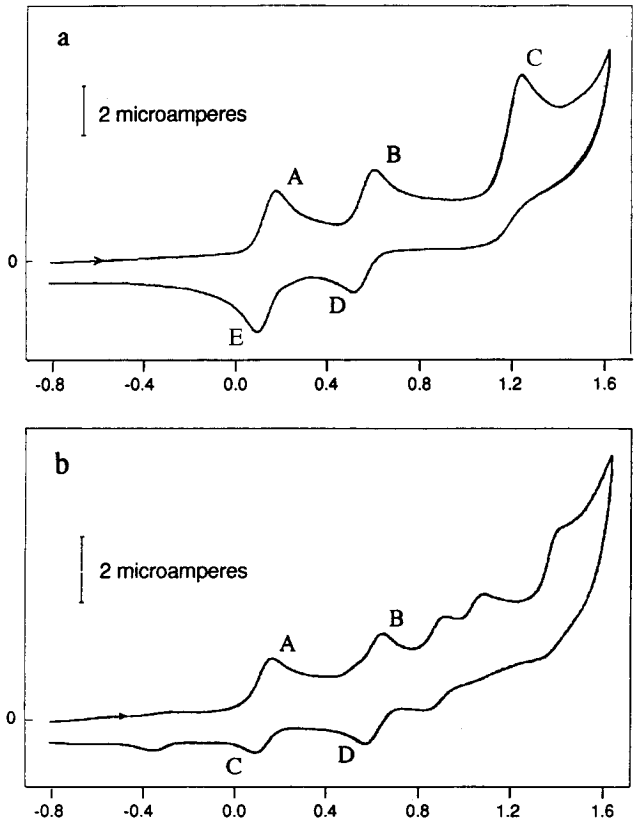

Figure 6. Cyclic voltammograms of 5×10^{-4} M solutions of (a) $[Rh_4(\mu\text{-}PyS_2)_2(cod)_4]$ (**1**) and (b) $[Ir_4(\mu\text{-}PyS_2)_2(cod)_4]$ (**4**) in CH_2Cl_2/0.1 M Bu_4NPF_6 at the scan rate 0.1 V s^{-1}.

waves are associated to two different electrogenerated species. The location of the two main oxidation waves for complex **6** shifted 460 and 250 mV to higher potentials than those observed for **1** and **3**, respectively, is in agreement with the greater π-acidity of the carbonyl ligands when compared with tfbb and cod.

Replacement of carbonyl ligands by less strong π-acceptor ligands as triphenylphosphine should increase the electronic density on the rhodium atoms, and the resulting complex should be easier to oxidize and harder to reduce. As expected, the cyclic voltagram of $[Rh_4(\mu\text{-}PyS_2)_2(CO)_4(PPh_3)_4]$ (**7**) in dichloromethane shows anodic processes shifted negatively from those observed for **6**. In fact, two well-defined peak systems are observed at -0.06 and $+0.36$ V together with several irreversible oxidations at $+0.60$, $+0.83$, and $+1.02$ (at 0.1 V s^{-1}). Analysis of the two first waves with scan rates ranging from 50 to 300 mV s^{-1} indicates that they are quasireversible electron transfers complicated by the following chemical reaction.[42]

The cyclic voltagram of $[Ir_4(\mu\text{-}PyS_2)_2(cod)_4]$ (**4**) in dichloromethane is rather complex and involves five subsequent anodic processes (Figure 6b). Analysis of the main peak systems A/C and B/D follows the reversibility criteria above described,[40] and hence, the anodic processes at $E_{1/2} = 0.08$ V and $E_{1/2} = 0.53$ V should correspond to reversible one-electron oxidations assigned to the formation of the mono-$[Ir_4(\mu\text{-}PyS_2)_2(cod)_4]^+$ and dicationic $[Ir_4(\mu\text{-}PyS_2)_2(cod)_4]^{2+}$ species having the cores $[Ir_4]^{5+}$ ($Z = +1$) and $[Ir_4]^{6+}$ ($Z = +2$), respectively. The anodic processes at $+0.84$, $+0.99$, and $+1.30$ V (at 0.1 V s^{-1}) correspond to irreversible oxidations. On reversal of the scan, reduction waves at $+1.2$, $+0.73$, and -0.37 V are observed, which arise from the reduction of previously oxidized species; in addition, the cathodic response shows also an irreversible reduction step at -1.12 V (not shown in Figure 6b).

On sight of these electrochemical features, the rhodium and iridium diolefinic complexes **1**, **3**, and **4** are the best candidates to undertake the chemical synthesis of the mono- and dicationic species since they undergo two reversible oxidation processes at formal electrode potentials which are accessible by chemical reagents. For each complex the two oxidation waves are separated approximately by $\Delta E^\circ = 0.4$ V (ΔE° = difference between the formal potentials of the two one-electron-oxidation steps), suggesting that the metals are communicating, since otherwise both oxidation waves should move closer together as has been found in dinuclear ferrocenyl derivatives.[43] With regard to the chemical synthesis, the monocationic species should be stable with respect to disproportionation since a large wave separation is observed. According to the Gagné's suggestions for dinuclear complexes[44] if one considers the following comproportionation equilibrium between tetranuclear complexes:

$$[M_4] + [M_4]^{2+} \rightleftharpoons 2\,[M_4]^+$$

the equilibrium constant K_{com} can be estimated as a function of ΔE°. In our complexes the obtained values are $K_{com} = 1.2 \times 10^7$ (**1** and **3**) and 4.1×10^7 (**6**). Although structural changes and several effects are reflected in K_{com} through changes in ΔE°, the electronic delocalization of the positive charge over all four metal atoms in the monocation enhances its stability, resulting in higher ΔE°. Large values of K_{com} (10^{34}) are due to the special stability of the delocalized valence. When no interaction takes place between the metals, $K_{com} = 4$ on the basis of statistical distribution of charges and results in a ΔE° value of 0.036 V and a single voltammetric wave.[44] Similar values of K_{com} to those found for our complexes have been found for tetranuclear Mo and Wo complexes[5c] and for the mixed-valence ion $[(NH_3)_5Ru(pyrazine)Ru(NH_3)_5]^{5+}$, which exhibits electronic delocalization; the reported Ru(III)−Ru(II) reduction potentials[45] for Ru(III)−Ru(III) → Ru(III)−Ru(II) → Ru(II)−Ru(II) gives $\Delta E^\circ = 0.39$ and $K_{com} = 4 \times 10^6$. For our complexes extensive delocalization of the charge between the metal centers occurs. Therefore, the removal of electrons should occur from the highest occupied molecular orbital delocalized over the tetrametallic core.

Acknowledgment. We thank DGICYT (Projects PB92 86-C02-02 and PB94-1186) and CICYT and Generalitat de Catalunya (Project QFN92-4311) for financial support and Diputacion General de Aragón for a fellowship (to M.A.C.).

Supporting Information Available: Tables of anisotropic displacement parameters, atomic coordinates for hydrogen atoms, full experimental details of the X-ray studies (Tables S1−S3), bond distances, angles, and interatomic distances and figures of the full assignment of the protons of the COSY spectra (Figures 3 and 4) with overlays superimposed (23 pages). Ordering information is given in any masthead page.

IC950849U

(42) Bianchini, C.; Frediani, P.; Laschi, F.; Meli, A.; Vizza, F. *Inorg. Chem.* **1990**, *29*, 3402.
(43) Geiger, W. E.; Connelly, N. G. *Adv. Organomet. Chem.* **1985**, *24*, 87.
(44) Gagné, R. R.; Spiro, C. L.; Smith, T. J.; Hamann, C. A.; Thies, W. R.; Shiemke, A. K. *J. Am. Chem. Soc.* **1981**, *103*, 4073.
(45) (a) Elias, J. H.; Drago, S. R. *Inorg. Chem.* **1972**, *11*, 415. (b) Creutz, C.; Taube, H. *J. Am. Chem. Soc.* **1973**, *95*, 1086.